Photoperturbation of the Heme a_3-Cu_B Binuclear Center of Cytochrome *c* Oxidase CO Complex Observed by Fourier Transform Infrared Spectroscopy

Sungjo Park,* Lian-Ping Pan,# Sunney I. Chan,# and James O. Alben*
*Department of Medical Biochemistry, The Ohio State University, Columbus, Ohio 43210, and #A. A. Noyes Laboratory of Chemical Physics, California Institute of Technology, Pasadena, California 91125 USA

ABSTRACT Purified cytochrome *c* oxidase CO complex from beef heart has been studied by Fourier transform infrared absorbance difference spectroscopy. Photolysis at 10–20 Kelvin results in dissociation of a_3FeCO, formation of Cu_BCO, and perturbation of the a_3-heme and Cu_B complex. The vibrational perturbation spectrum between 900 and 1700 cm^{-1} contains a wealth of information about the binuclear center. Appearance in infrared photoperturbation difference spectra of virtually all bands previously reported from resonance Raman spectra indicate the importance of polarization along the 4-vinyl:8-formyl axis, which results in the reduction of heme symmetry to C_{2v}. Frequency-shifted bands due to the 8-formyl and 4-vinyl groups of the a_3-heme have been identified and quantitated. The frequency shifts have been interpreted as being due to a change in porphyrin polarization with change in spin state of the iron by photodissociation of CO or perturbation of the Cu_B coordination complex.

INTRODUCTION

Cytochrome *c* oxidase is the terminal respiratory enzyme in eucaryotic plants and animals. It catalyzes the reduction of molecular oxygen to water and conserves the chemical energy for use in cellular processes. It consists of two iron porphyrin (heme *a* and a_3) and two copper sites (Cu_A and Cu_B) (Wikstrom et al., 1981; Babcock and Wikstrom, 1992; Chan and Li, 1990). The heme *a* and Cu_A participate in electron transfer from cytochrome *c* to the binuclear site, which consists of heme a_3 and Cu_B. Dioxygen is bound and reduced to water at the a_3Fe-Cu_B binuclear site. The molecular interactions between metal-bound axial ligand and its molecular surroundings provide the chemical basis for biological control of respiratory processes (Woodruff et al., 1991; Chan and Li, 1990).

The formyl group at the 8-position on the porphyrin ring of heme a_3 provides a molecular probe of such interactions. Although the formyl group is a weak scatterer, it has been studied by resonance Raman spectroscopy, and frequency assignments have been made from heme A and from purified cytochrome *c* oxidase (Salmeen et al., 1973; Callahan and Babcock, 1983; Babcock and Callahan, 1983; de Paula et al., 1990; Ching et al., 1985; Argade et al., 1985; Sassaroli et al., 1988; Choi et al., 1983). Suggestions have been presented that the formyl group of heme A in cytochrome oxidase may be hydrogen bonded to a protein group, and/or the formyl group may be sensitive to conformational changes in the protein (Sassaroli et al., 1988). Such interactions may affect the chemical reactivity of ligands coordinated to the iron.

Fourier transform infrared (FTIR) spectroscopy (Alben and Fiamingo, 1984) has been used to monitor and characterize the heme a_3 and Cu_B binuclear site after photodissociation of the carbon monoxide from the $a_3$heme-CO complex. The photodissociated CO forms a complex with Cu_B that is stable at temperatures below 140 Kelvin (Alben et al., 1981, 1982a,b; Fiamingo et al., 1982, 1986). Photodissociation of the a_3FeCO complex of cytochrome *c* oxidase has provided essential information about structural interactions at the a_3Fe:Cu_B site. Measurements at low temperature (10–180 Kelvin) by Fourier transform infrared spectroscopy provided the first observation of Cu_BCO complex (Alben et al., 1982a,b) and demonstrated that an unhindered path exists between a_3Fe and Cu_B. Photodissociation of a_3FeCO results in very rapid formation of Cu_BCO, even at 10 Kelvin, and thermal dissociation of the Cu_B complex proceeds at measureable rates above 140 Kelvin with reformation of the a_3FeCO complex. In the reduced CO complex, a_3Fe and Cu_B must be close enough to provide a clear path between them, but far enough apart so that the 2.5 cm^{-1} bandwidth of a_3FeCO at 1963 cm^{-1} is not broadened by interaction with the adjacent Cu_B complex. We therefore estimated the distance between these metal centers to be 4–6 Å in the reduced CO complex (Fiamingo et al., 1982; Alben et al., 1981). Recent crystallographic studies indicate a a_3Fe-Cu_B distance of 5.2 Å in the *Pseudomonas denitrificans* cytochrome *c* oxidase (Iwata et al., 1995) and 4.6 Å in the bovine oxidase (Tsukihara et al., 1995).

In this study, we optimized sampling conditions and instrumentation to permit observation of infrared perturbation spectra of cytochrome *c* oxidase in aqueous solution between 950 cm^{-1} to 1700 cm^{-1} at a high signal-to-noise ratio. Photodissociation of the cytochrome a_3FeCO perturbs

Received for publication 10 October 1995 and in final form 2 May 1996.
Address reprint requests to Dr James O. Alben, Department of Medical Biochemistry, Ohio State University, 1645 Neil Avenue, Columbus, OH 43210. Tel.: 614-292-4876; Fax: 614-292-4118; E-mail: jim@biospec.bsl.ohio-state.edu.

Dr. Park's present address is Department of Biochemistry and Molecular Biology, Mayo Foundation, 200 First St. SW, Rochester, MN 55905.

0006-3495/96/08/1036/12 $2.00

the porphyrin ring and substituents such as 8-formyl and 4-vinyl groups, resulting in frequency shifts that are observed by absorbance difference spectroscopy (light − dark). A preliminary report has appeared (Park et al., 1992).

MATERIALS AND METHODS

Beef heart cytochrome *c* oxidase was isolated by the method of Hartzell and Beinert (Hartzell and Beinert, 1974; Pan et al., 1991). After the addition of 1 equivalent of ascorbate and 0.05 equivalent of cytochrome *c*, the enzyme samples were thoroughly degassed on a high-vacuum apparatus and subsequently exposed to 1 atmosphere of CO gas (Matheson, 99.5%) at 4°C overnight. The enzyme preparation was stored in liquid nitrogen until it was used. Visible spectra of cytochrome *c* oxidase at 4°C were obtained with a Cary model 17DX spectrometer.

All infrared spectra were recorded at 0.5 cm^{-1} resolution with a Mattson Sirius 100 FTIR interferometer, which was fitted with a liquid nitrogen-cooled photovoltaic (HgCd)Te detector for measurements below 1800 cm^{-1}, or with a liquid nitrogen-cooled InSb detector for measurements above 1800 cm^{-1}. The detectors were fitted with appropriate low-pass optical filters to limit the optical bandpass to the spectral region of interest and to improve signal-to-noise. Cytochrome *c* oxidase CO samples were pressed between BaF_2 windows with an optical path of 8.8 μm. Low temperature was obtained by use of a Lake Shore Cryotronics closed-cycle helium refrigerator (model LTS-21-D70C). Cryostat cell temperature was measured by use of a Lake Shore Cryotronics digital thermometer (model DRC-70) with a calibrated silicon diode probe. Photolysis made use of a 500-W tungsten lamp focused through a slide projector and passed through a water filter (2 cm) to remove infrared radiation beyond 1.2 μm. Photodissociation absorbance difference spectra (light − dark) were obtained from the ratio of single-beam spectra in the absence (dark) and in the presence (light) of visible radiation. The optical bench was flushed with highly dried compressed air to remove water vapor absorption that occurs in the infrared beam path. Residual water vapor spectral contributions were clearly distinguished from absorption bands due to perturbations of the sample by use of 0.5 cm^{-1} resolution for all infrared measurements. Residual water vapor contributions in the midinfrared were reduced by scaled absorbance subtraction of a separately collected water vapor spectrum and were distinguished from noise by their frequencies.

Imidazole was a product of Eastman Co. ImidazoloCu(II) perchlorate was a gift of Dr. Noel J. Farrier. All other chemicals were reagent grade and used as received.

RESULTS

Photodissociation of the cytochrome *c* oxidase carbon monoxide complex at cryogenic temperatures can be used to probe molecular structure and structural interactions at the heme a_3-Cu_B binuclear center (Alben, 1996). Ligands to both metals are expected to be perturbed as a result of dissociation of a_3FeCO and formation of Cu_BCO. The affected ligands are illustrated in Fig. 1, which was adapted from the crystal structures (Iwata et al., 1995; Tsukihara et al., 1995). Note that transmembrane helices of subunit 1 are arranged counterclockwise around the binuclear center (Iwata et al., 1995), rather than clockwise, as previously represented (Garcia-Horsman et al., 1994; Alben, 1996).

Purified cytochrome *c* oxidase was characterized by visible and infrared spectroscopy of the carbon monoxide complex. The visible spectrum (Fig. 2) is characteristic of the reduced CO complex. The bands at 430.8 and 594.3 nm are characteristic of the a_3FeCO complex, whereas the absorptions at 443.5 and 603.3 nm are characteristic of the reduced cytochrome *a*. The visible spectrum in Fig. 2 was recorded after the infrared measurements in Fig. 4, *a–c*, and thus represents the final state of the enzyme.

Photodissociation of the purified cytochrome oxidase CO complex at 12 Kelvin yielded infrared spectra of the CO complexes (Fig. 3) similar to those previously reported for beef heart mitochondria, rat heart myocytes, and purified cytochrome oxidase (Fiamingo et al., 1982, 1986; Dyer et al., 1989). Alpha-form conformers at 12 Kelvin exhibit an absorption due to a_3FeCO at 1962.5 cm^{-1} and a split Cu_BCO band at 2054.8 and 2064.8 cm^{-1}, and beta-forms exhibit a_3FeCO bands at 1944.1, 1948.2, and 1957 cm^{-1}, and a single Cu_BCO band at 2041.3 cm^{-1}. The ratio of beta/alpha-form (0.079) was less than that observed with beef heart tissue or myocytes isolated from rat heart (Fiamingo et al., 1986), but similar to that observed in mito-

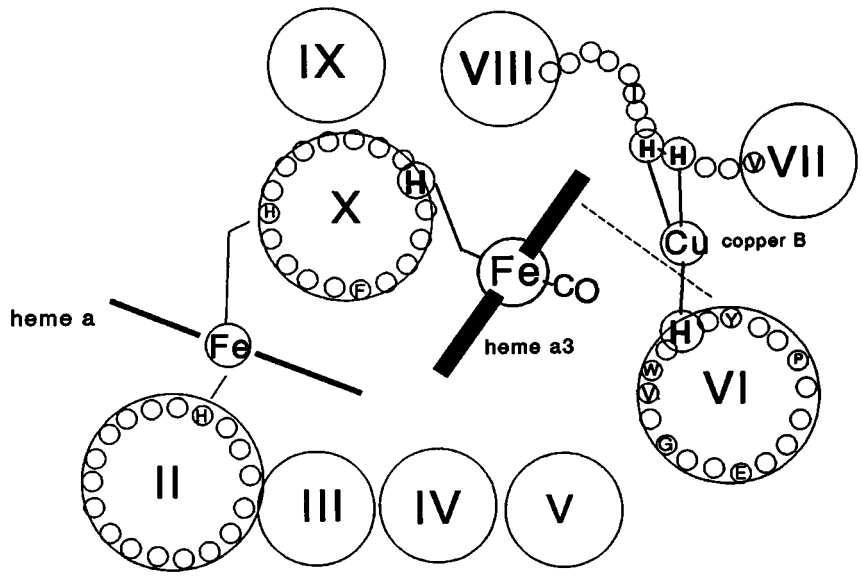

FIGURE 1 Model of heme centers and Cu_B in cytochrome *c* oxidase, showing transmembrane helices of subunit I, viewed perpendicular to the membrane surface from the cytoplasmic (or periplasmic) side. Adapted from Iwata et al. (1995). Heme a_3, Cu_B, and coordinated histidines are emphasized.

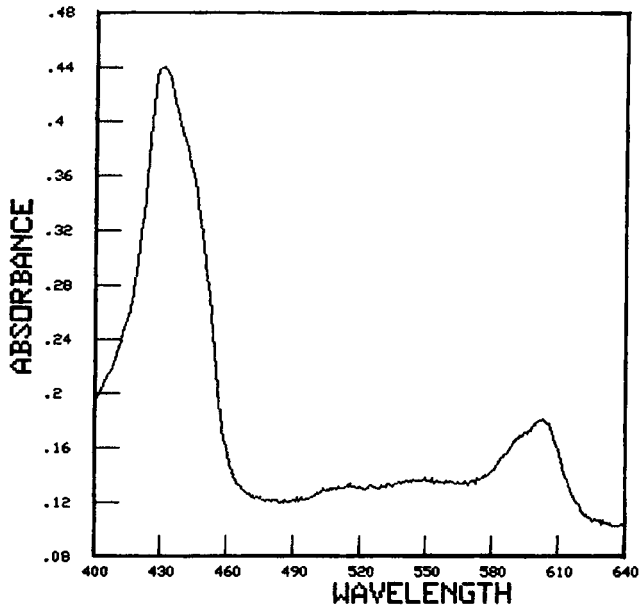

FIGURE 2 Room-temperature visible spectrum of cytochrome *c* oxidase CO complex after low-temperature photodissociation studies illustrated in Figs. 3 and 4.

chondria (Fiamingo et al., 1982) isolated from beef heart. Similar spectra were previously measured with dithionite-reduced and autoreduced (mixed valence) CO complexes of purified cytochrome *c* oxidase (D. Bickar et al., unpublished data). The frequency accuracy is limited only by noise and baseline uncertainty, because the instrumental inaccuracy was measured to be $+0.024 \pm 0.02$ cm^{-1} (1:100,000) corrected to vacuum, by comparison of spectra of carbon monoxide gas at low partial pressure with literature values (Cole, 1977). Sample composition and concentration (3.3 mM, 7.0 μm optical path) were determined from the 12 Kelvin photodissociation difference spectrum of the iron carbonyl at 1962.5 cm^{-1} (Fig. 3), assuming an integrated absorptivity of 28 mM^{-1} cm^{-2} (Yoshikawa et al., 1977). These sampling conditions resulted in single-beam spectra with transmission greater than 10% of the maximum from 900-1800 cm^{-1}, and the signal-to-noise illustrated in Fig. 4, *a–c*.

After collection of the cytochrome oxidase CO spectra in Fig. 3, the cryostat was moved to a second Mattson interferometer fitted with a photovoltaic (HgCd)Te detector for measurements through the amide and fingerprint spectral regions (900–1800 cm^{-1}). The sample temperature was raised to 200 Kelvin for 20 min to thermally dissociate the Cu_BCO with reformation of a_3FeCO, and then recooled to 13 Kelvin. Infrared data collected before and after a 10-min photodissociation show perturbations of many bands in the absorbance difference spectrum (Figs. 4, *a–c*). The spectral observations were replicated an additional 11 times by relaxation at 200 Kelvin, cooling to 8–20 Kelvin, and signal averaging between 2,048 and 16,384 interferograms each before and after a 10-min photolysis. The absorbance difference bands were well reproduced. A second sample yielded a similar difference spectrum.

The Mattson Sirius 100 infrared interferometer in our laboratory is able to collect data in both forward and reverse directions of mirror motion, to produce a separate signal-averaged interferogram from each direction. The signal-averaged interferograms are highly interlaced in time, but are independent measurements that are separately Fourier transformed and phase corrected for each direction of the moving mirror. Light/dark absorbance difference spectra obtained separately from forward and reverse mirror directions were averaged to reduce random noise by $\sqrt{2}/2$ (upper curve in Fig. 4, *a–c*). Forward minus reverse absorbance difference spectra (lower trace) contained no spectral information, and only the random noise and phase error contributions from each data collection. The random noise in the lower trace ($\sqrt{2} \times$ each spectrum) is thus twice that in the upper trace. The spectra in Fig. 4, *a–c*, are clearly distinguished from random noise or phase errors. Residual atmospheric water vapor contributions exhibit resolution-limited bandwidths (0.5 cm^{-1}) and are clearly distinguished from vibrational modes due to the sample. Phase errors can produce "false bands" not due to molecular changes in the sample associated with photodissociation. Noise and phase errors are accentuated in spectral regions of low light transmission, such as the amide region. We therefore limit interpreted data to regions where light transmission is greater than 12% of the maximum single-beam spectrum, and sample perturbation bands are large relative to noise or residual water vapor absorptions. Peak/peak noise was 150 microabsorbance at 1660 and 1550 cm^{-1} (at amide I and II), 50 microabsorbance at 1600 cm^{-1}, and 25 microabsorbance from 1500 to 940 cm^{-1}.

Midinfrared photodissociation difference spectra are illustrated in Fig. 4, *a–c*, and summarized in Table 1. One is immediately struck by the large number of bands that shift either frequency or amplitude with photodissociation. These bands are highly reproducible and clearly distinguished from instrumental or sampling artifacts. Cytochrome *c* oxidase has not previously been studied by midinfrared spectroscopy but has been extensively studied by resonance Raman spectroscopy. Table 1 includes a detailed comparison of infrared difference spectra with Raman spectra of cytochrome *c* oxidase and of model compounds. Although band intensities differ between infrared and resonance Raman, virtually every Raman-active band also appears to be present in the infrared difference spectra, as a difference band maximum or minimum. In addition, several infrared bands are present that are not reported in the Raman spectra. We will show that many of these additional bands can be accommodated by methyl or methylene substituents on the porphyrin ring of cytochrome a_3, or by histidines coordinated to a_3Fe or to Cu_B.

Fig. 4 and Tables 1 and 2 show large amplitude difference bands (greater than 1 milliabsorbance, peak/peak) centered near 1662 cm^{-1}, 1368 cm^{-1}, 1304 cm^{-1}, 1236 cm^{-1}, and 1082 cm^{-1}, in addition to many smaller amplitude bands.

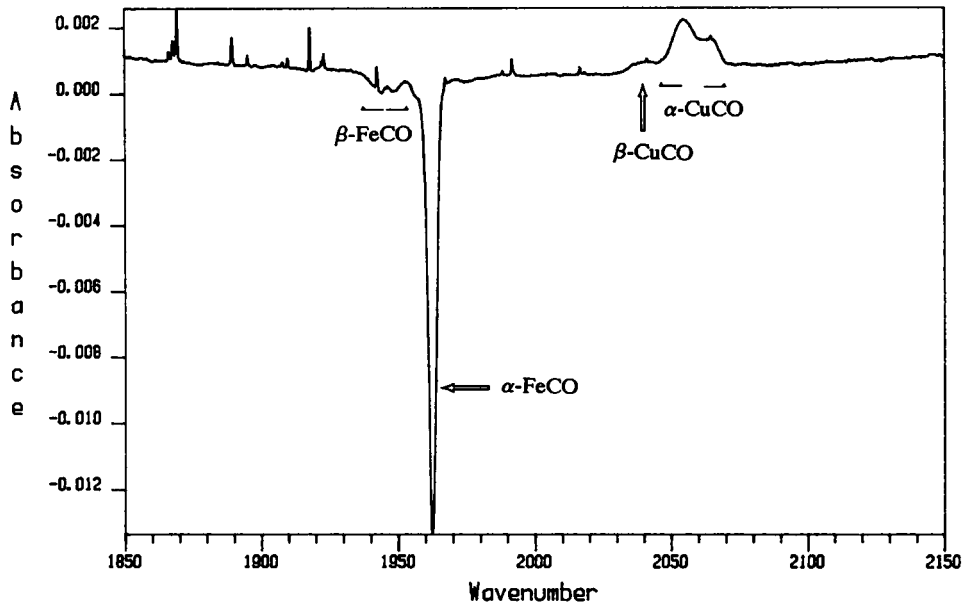

FIGURE 3 Fourier transform infrared absorbance difference spectrum of the CO complex of cytochrome *c* oxidase at 12 K, "after" minus "before" photodissociation (light minus dark).

Frequency-shifted bands (Alben and Fiamingo, 1984; Alben and Bare, 1978) (e.g., 1662, 1368, 1304, and 1082 cm^{-1}) have an appearance roughly similar to the first derivative of an absorption band and are identified by the frequency of the zero crossing and the amplitude of the absorption difference (Fig. 5, Table 1). Other perturbations may result in a change in absorptivity (e.g., 1236 cm^{-1} band), so the difference band is only pointed either up or down, or in a change in bandwidth, which results in an appearance roughly similar to a second derivative or to a sin *x*/*x* function. The largest amplitude first derivative-shaped band is centered at 1662 cm^{-1} (ΔA = 2.6 milliabsorbance, mA) and is assigned to a frequency-shifted νCO of the 8-formyl group of the cytochrome a_3 heme, in agreement with resonance Raman assignments to heme A (Han et al., 1991; Argade et al., 1985; Wilson et al., 1988) and infrared spectra of formyl-substituted porphyrins (Alben et al., 1973). Additional bands appear at 1081.6 cm^{-1} (ΔA = 1.16 mA), 1304.2 cm^{-1} (ΔA = 1.05 mA), 1368.5 cm^{-1} (ΔA = 1.04 mA), and 1629.7 ± 0.3 cm^{-1} (ΔA = 0.85 mA). We assign the band at 1081.7 cm^{-1} to a $\delta_{as}(=CH_2)$ rocking mode and the 1629.7 cm^{-1} band to a $\nu(C=C)$ stretching mode of the 4-vinyl group of the a_3-heme, in agreement with previous work (Alben et al., 1968; Choi et al., 1982a,b). The band at 1304.2 is consistent with a vinyl δ(CH) bending mode (Ogura et al., 1990). The band at 1368.5 cm^{-1} may be associated with porphyrin modes, ν41 and ν4. We can associate the band near 1335 cm^{-1} with a vinyl $\delta_s(=CH_2)$ bending mode. The strong downward-pointing difference band at 1236 cm^{-1} is ligand sensitive and most pronounced in porphyrin-Fe-CO complexes. We therefore assign it to an a_3Fe-imidazole mode coupled to CO.

The absorbance difference spectrum (Fig. 4 *a*) was analyzed (Alben and Fiamingo, 1984; Alben and Bare, 1978; Laane and Kiefer, 1980; Laane, 1981; Rousseau, 1981) to measure the frequency shift of the formyl band upon photodissociation. This is possible because the symmetry of the frequency-shifted band suggests negligible overlap with adjacent bands. The frequency of the zero crossing can be precisely measured and represents the mean of the band center frequencies before and after photodissociation. Analysis of the frequency shift (Fig. 5) observed by absorbance difference spectroscopy depends upon knowledge of the absorbance maximum (A_o) of the frequency-shifted band, the half-bandwidth (Γ = FWHH), and the shape of the band (e.g., Gaussian and Lorentzian), in addition to the observed peak-to-trough absorbance difference (ΔA = 0.0026 = 2.6 mA). We have not directly observed the total infrared absorption band due to the 8-formyl group (it is highly overlapped with the amide I band), but we can approximate the required information by comparison with benzaldehyde in the following manner. We assume that the integrated absorptivity (B) and type of band shape (Gaussian, Lorentzian, etc.), but not A_o or Γ, are the same for the formyl groups of heme A and benzaldehyde. Then from the Beer-Lambert relation and letting band area $\propto A_o \cdot \Gamma$, it follows that $A_o\Gamma_o/A_1\Gamma_1 = c_o l_o/c_1 l_1$, and $A_o = (A_1\Gamma_1/\Gamma_o)(c_o l_o/c_1 l_1)$, where subscripts 1 and o refer to benzaldehyde and cytochrome *c* oxidase, and c and l refer to concentration and pathlength, respectively. For this sample of cytochrome a_3 (Figs. 2, 3, and 4 *a–c*), $A_o = 0.055/\Gamma$. Limiting values of the a_3-heme formyl bandwidth (Γ = FWHH) are given by the following inequalities (Alben and Fiamingo, 1984): $\Gamma \geq \Delta\nu_{1/4}$; $\Gamma_g \leq \delta/0.849$ (Gaussian), or $\Gamma_l \leq \delta/0.577$ (Lorentzian); and $\Delta\nu_o \leq \delta$, where these parameters are defined in Fig. 5. For cytochrome *c* oxidase, $\Delta\nu_{1/4}$ = 4.0 cm^{-1}, and δ = 5.2 cm^{-1}. These relations lead to limiting values of Γ = 4 to 6 cm^{-1} (Gaussian) and Γ = 4 to 9 cm^{-1} (Lorentzian) for the a_3-formyl group, and to center frequency shifts $\Delta\nu_o$

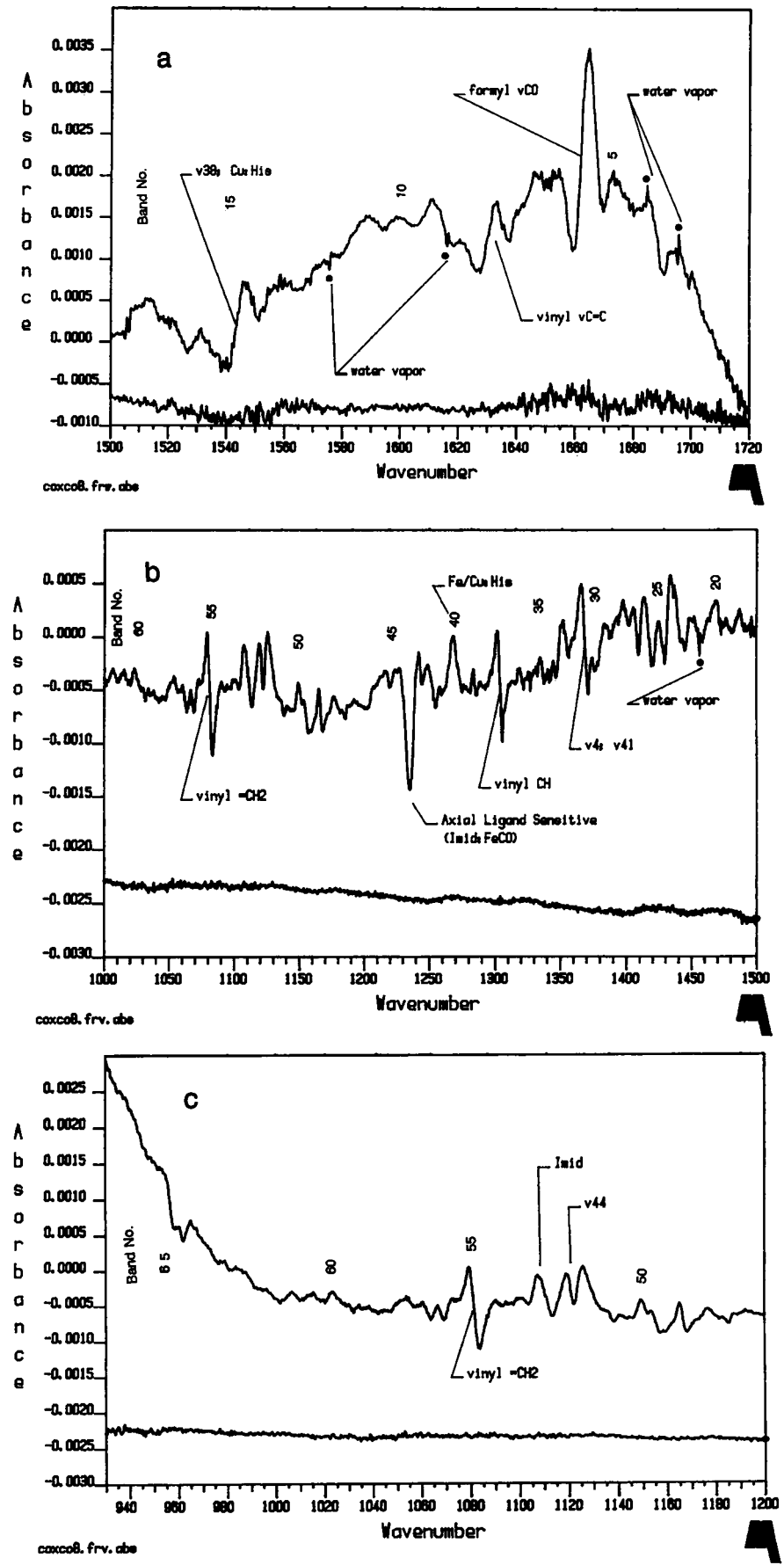

FIGURE 4 The photoperturbation infrared spectrum (light minus dark) of heme a_3 of cytochrome *c* oxidase at 13 Kelvin. Absorbance difference spectra (*L/D*) computed from 8,192 interferograms measured during forward motion of the interferometer mirror were averaged with difference spectra computed from interograms measured during the reverse motion of the interferometer mirror (see text). The difference between absorbance difference spectra (*L/D*) from the two mirror directions (*lower trace*) contains no signal, but only random noise. Band numbers refer to tabulations (Tables 1 and 2). (*a*, *b*, and *c*) Expanded spectral regions.

TABLE 1 Infrared absorbance difference spectra of cytochrome c oxidase CO complex

	FTIR light/dark (this work)					Literature*		Literature#	
Band no.	Minimum (dark) (cm^{-1})	Maximum (light) (cm^{-1})	Midpoint (cm^{-1})	Absorbance (ΔmA) (max − min)¶	Suggested assignment§	Cytox a_3CO; RR 413.1 nm	Cytox a^{2+}; RR 441.6 nm	Cytox (red) RR	Cytox (oxid) RR
1a		2065		2.3	Cu_BCO (α)				
1b		2055		1.5	νCO (split)				
2		2040		0.9	Cu_B (β) νCO				
3	1962.8			18.9	a_3FeCO, (α) νCO				
4	1691	1686		0.5					
5	1670	1674		0.28	νC=O				1676
6	1660	1664.5	1661.9	2.60	formyl νC=O	1666		1667	
6a									1650
7	1638				ν10				
8	1627	1633	1629.7	0.85	vinyl νC=C		1625	1624	1626
9	1619	1612		0.6	νC=C; ν10?	1618		1611	1618
10		1600			ν10		1609		
11	1595			0.08					
12	1580	1589			ν2; ν37	1585	1586	1588	1588
13	1565				ν37;ν38	1567	1568	1574	1573
14	1551								
15	1540	1546	1543	1.0	ν38	1541		1547	
16	1527	1531		0.2	ν38; ν11			1520	1520
17		1513			ν11; ν3	1516	1517		1504
18	1493	1487		0.25	ν3		1493	1493	
19	1481	1478							
20	1475	1469		0.30	ν28	1469	1464	1470	1476
21	1458				ν39; $\delta_{as}CH_3$; δCH_2 (ring)				
22	1445	1449		0.32	ν28				1446
23	1442			0.64	ν40; δ_sCH_3			1441	
24	1429	1434		0.75					
25	1421	1425		0.42	δCH_2(CO)				
26	1410	1414		0.55					
27	1402	1406		0.201					
28		1398		0.24	ν20, 29; vinyl δCH=	1398	1399	1397	1395
29	1388	1384		0.10					
30	1376	1374		0.14	ν4, 41				
31	1371.2	1365.9	1368.5	1.04	ν41; ν4	1368			1371
32	1356	1352		0.36	ν4		1354	1358	
33	1348	1344		0.14					
34	1343	1341		0.16					
35	1338	1335		0.24	vinyl δ_s=CH_2	1328	1331	1334	1336
36	1327								
37	1322	1319		0.12					
38	1305.8	1301.7	1304.2	1.05	vinyl δCH=; ν21	1306	1305	1306	1310
39	1286	1284		0.26	ν42	1286	1289	1293	1292
40	1275	1269		0.50					
41	1261	1258		0.08					
42	1255	1250		0.40		1255			
43	1245	1242		0.30	ν5 + ν9	1244	1246	1251	1250
44	1236			1.14	Imid:FeCO				
45	1221	1217		0.16	Formyl νC_β-CO; ν13	1227	1226	1229	1228
46	1203								
47	1186	1177		0.20	ν30	1182	1181	1185	1184
48	1169	1165		0.42	ν30			1164	1170
49	1159				ν30	1159			
50	1157	1150		0.48					
51	1138				ν43	1133	1131	1133	1131
52	1123	1126		0.56					
53	1114	1119		0.60	ν44	1116	1113		
54	1104	1108		0.44					

TABLE 1 Continued

	FTIR light/dark (this work)					Literature*		Literature#	
Band no.	Minimum (dark) (cm^{-1})	Maximum (light) (cm^{-1})	Midpoint (cm^{-1})	Absorbance (ΔmA) (max − min)¶	Suggested assignment§	Cytox a_3CO; RR 413.1 nm	Cytox a^{2+}; RR 441.6 nm	Cytox (red) RR	Cytox (oxid) RR
55	1083.8	1079.5	1081.6	1.16	Vinyl δ_{as}=CH_2		1087		
56	1070	1073		0.35					
57	1069	1067		0.21					
58	1064	1061		0.25					
59	1057	1054		0.16					
60	1020	1024		0.14					
61	1002	1007		0.14	Vinyl γCH=				
62					ν45			976	
63	962	965		0.52				965	
64	959								
65	947	954		0.90					
66				0.35	ν46			938	

*Argade et al. (1985).
#Choi et al. (1983).
§Assignments were adapted from resonance Raman studies (Argade et al., 1985; Choi et al., 1983) and this work.
¶Delta absorbance (maximum − minimum) is given in units of milliabsorbance (mA) = $A \times 10^{-3}$.

= 0.27 to 0.6 cm^{-1} (Gaussian), or $\Delta\nu_o$ = 0.3 to 1.5 cm^{-1} (Lorentzian).

Infrared photoperturbation difference spectra are compared with resonance Raman spectra (Argade et al., 1985; Choi et al., 1983) of cytochrome *c* oxidase derivatives in Table 1, and with infrared and Raman spectra of model compounds (imidazole (this work and Colombo et al., 1974; Walters and Spiro, 1983) and heme A (Choi et al., 1983) complexes) in Table 2.

Assignment of specific vibrational modes to many bands is somewhat uncertain, as indicated by multiple designations in Table 1. These assignments were based on comparisons of resonance Raman spectra (Argade et al., 1985; Choi et al., 1983) with normal modes calculated for nickel octaethylporphyrin, which has D_{4h} symmetry. Only 18 E_u (in plane) and 6 A_{2u} (out of plane) vibrational modes are expected to be infrared active in D_{4h} symmetry. Table 1 shows numerous infrared difference bands (~62 between 1700 and 940 cm^{-1}), many of which correspond closely to assigned Raman active modes (A_{1g}, B_{1g}, A_{2g}, and B_{2g}). Absorption bands that correspond to virtually every reported Raman transition are observed in the infrared perturbation spectra (Table 1). This observation is consistent with a symmetry of heme a that is much lower than D_{4h} and is fully consistent with C_{2v} symmetry. The reduced symmetry appears to result directly from the strong dipole moment produced by the electron-withdrawing formyl substituent at the 8-position in heme a, coupled to the polarizable vinyl substituent at the 4-position, which splits heme A into two electronically similar mirror images. A_{1g} and B_{1g} modes become A_1 modes in C_{2v} symmetry, A_{2g} and B_{2g} become B_2 modes, and E_u modes are divided between A_1 and B_2 (Kitagawa and Ozaki, 1987). Both A_1 and B_2 are expected to be infrared active, as observed in Table 1. We therefore compare the infrared perturbation bands with assignments from Raman spectra of the CO complex and reduced cytochrome *c* oxidase complexes in Table 1. Of the 62 infrared perturbation bands listed below 1800 cm^{-1}, as many as 29 may have counterparts in Raman spectra. These bands include vibrations associated with the 4-vinyl and 8-formyl substituents of heme A, but no ring-bound methyl or propionate groups or axial residues coordinated to the iron. Both of the latter groups are expected to be infrared active but not resonance enhanced in Raman spectra. Asymmetric bending modes ($\delta_{as}CH_2$ and $\delta_{as}CH_3$) for heme substituents have been reported between 1465 and 1433 cm^{-1}, and symmetric modes at 1359 and 1382 cm^{-1} (Alben, 1978; Alben and Fiamingo, 1984); these may contribute to the cytochrome oxidase photoperturbation spectra in Table 1.

Infrared photoperturbation spectra are compared with model compounds in Table 2. Spectra of $(imidazolo)_xCu(II)$ perchlorate complexes provide a model for the histidino-Cu_B complex in cytochrome *c* oxidase and are similar to that of aqueous imidazole at pH 10.3. Monoimidazolopentacyanoferrate (Walters and Spiro, 1983) and mono- and bisimidazo Fe(II) porphyrin A serve as models for heme a_3, whereas porphyrin A Fe(III)Cl is a heme A model with no axial imidazole and helps to distinguish vibrational modes due to imidazole or porphyrin (Choi et al., 1983). Approximately 16 Cu-imidazole modes and 9 Fe-imidazole modes have been observed and may contribute to the cytochrome *c* oxidase perturbation spectra. Although some of these overlap porphyrin vibrational modes, several appear to be sufficiently isolated to serve to distinguish Cu_B-histidine from a_3Fe-histidine vibrational modes.

Nineteen absorbance difference bands are listed in Table 2 for which no assignment is suggested. Some of these may represent local molecular interactions with the surrounding protein pocket that are perturbed by photodissociation at 8–20 K.

TABLE 2 Infrared absorbance difference spectra (light/dark) of cytochrome *c* oxidase

Cytochrome *c* oxidase CO (FTIR light/dark (this work)						Model compounds FT-IR (this work)				Literature*			Lit.#
Band no.	Minimum (dark) (cm^{-1})	Maximum (light) (cm^{-1})	Midpoint (cm^{-1})	Absorbance (ΔmA) (max − min)	Suggested assignment	Imidazole (aq.) pH 10.3	Imidazole (aq.) pH 5.3	$(ImH)_4$ Cu(II) ClO_4 (aq.)	$(ImH)_4$ Cu(II) ClO_4 Nujol	Pa Fe(III) Cl IR	$(ImH)_2$ Fe(II) Pa RR	2-MeIm Fe(II) Pa RR	(ImH) Fe(III) $(CN)_5$
1a		2055		2.3	Cu_BCO (α)								
1b		2065		1.5	νCO (split)								
		2040		0.9	Cu_BCO (β)								
					νCO								
3	1962.8			18.9	a_3FeCO, (α)								
					νCO								
4	1691	1686		0.5									
5	1670	1674		0.28	νC═O					1676			
6	1660	1664.5	1661.9	2.60	formyl								
					νC═Oν								
7	1638				ν10						1644	1645	
8	1627	1633	1629.7	0.85	vinyl					1628	1628	1624	
					νC═C								
											1623		
9	1619	1612		0.6	νC═C;						1620		
					ν10?								
10		1600			ν10						1614	1607	
11	1595			0.08							1593		
12	1580	1589			ν2; ν37					1580	1588	1578	
											1583		
13	1565				ν37; ν38						1574	1563	
14	1551							1547	1547				
15	1540	1546	1543	1.0	ν38; CuHis	1534	1538	1540	1542	1544	1546		
16	1527	1531		0.2	ν38; ν11;							1533	1530
					FeHis								
17		1513			ν11; ν3			1507	1513	1512	1504		1507
18	1493	1487		0.25	ν3; Imid	1488.6		1497	1497		1493	1496	
									1493				
19	1481	1478											
20	1475	1469		0.30	ν28; Imid			1475	1472		1469	1472	
21	1458				ν39;		1455						
					$\delta_{as}CH_3$;								
					δCH_2 (ring)								
22	1445	1449		0.32	FeHis; ν28							1443	1450
23	1442			0.64	ν40; δ_sCH_3					1439			
24	1429	1434		0.75	CuHis	1428.2		1430	1434				
25	1421	1425		0.42	$\delta CH_2(CO)$			1420					
26	1410	1414		0.55									
27	1402	1406		0.20									
28		1398		0.24	ν20, 29;						1392	1397	
					vinyl							1390	192
					δCH═								
29	1388	1384		0.10					1381				
30	1376	1374		0.14	ν4, 41				1375	1378			
31	1371.2	1365.9	1368.5	1.04	ν41; ν4				1367				
32	1356	1352		0.36	ν4						1359	1356	
33	1348	1344		0.14									
34	1343	1341		0.16									
35	1338	1335		0.24	vinyl					1338			
					δ_s═CH_2								
36	1327				Imid	1328.4	1325	1328	1330		1332	1330	1331
37	1322	1319		0.12				1313					
38	1305.8	1301.7	1304.2	1.05	vinyl				(1302)	1301	1308	1311	
					δCH═;						1305		
					ν21								
39	1286	1284		0.26	ν42			1285			1280	1287	
40	1275	1269		0.50	Fe/Cu:His				1627				1269
41	1261	1258		0.08		1259		1260		1260			
42	1255	1250		0.40	ν5 + ν9							1247	
43	1245	1242		0.30				1241					

TABLE 2 Continued

Cytochrome *c* oxidase CO (FTIR light/dark (this work)						Model compounds FT-IR (this work)				Literature*			Lit.#
Band no.	Minimum (dark) (cm^{-1})	Maximum (light) (cm^{-1})	Midpoint (cm^{-1})	Absorbance (ΔmA) (max − min)	Suggested assignment	Imidazole (aq.) pH 10.3	Imidazole (aq.) pH 5.3	$(ImH)_4$ Cu(II) ClO_4 (aq.)	$(ImH)_4$ Cu(II) ClO_4 Nujol	Pa Fe(III) Cl IR	$(ImH)_2$ Fe(II) Pa RR	2-MeIm Fe(II) Pa RR	(ImH) Fe(III) $(CN)_5$
44	1236			1.14	His:FeCO						1240	1232	
					Formyl νC_β-CO;						1226		
45	1221	1217		0.16	ν13			1227	1226		1220		
46	1203												1198
47	1186	1177		0.20	ν30								
48	1169	1165		0.42	ν30; Imid			1173	1167		1168	1174	
49	1159				ν30	1160							
50	1157	1150		0.48									
51	1138				ν43; FeHis	1135.5				1140	1133	1138	1142
52	1123	1126		0.56			1127				1128		
53	1114	1119		0.60	ν44				1114	1116		1119	
54	1104	1108		0.44	Fe/Cu:His	1097	1103	1102					1109
					vinyl								
55	1083.8	1079.5	1081.6	1.16	δ_{as}=CH_2						1084		
56	1070	1073		0.35	Imid			1073					1073
57	1069	1067		0.21		1067							
58	1064	1061		0.25									
59	1057	1054		0.16	Imid		1057						
60	1020	1024		0.14									
					Vinyl								
61	1002	1007		0.14	γCH=							1007	
62					ν45					998	995		983
63	962	965		0.52									
64	959												958
									952				
65	947	954		0.90	Imid				949				
66				0.35	Imid; ν46	935			931				

*Choi et al. (1983).
#Walters and Spiro (1983).

DISCUSSION

The photodissociation of CO in cytochrome *c* oxidase from a_3Fe to Cu_B at 8–20 K produces changes in molecular structure of both the a_3Feporphyrin and Cu_B coordination complexes, and thus in their infrared spectra. It provides a molecular selectivity that differs from other spectroscopic methods. It is highly specific to the a_3Fe-Cu_B binuclear center. Carbon monoxide diffusion through the protein between the binuclear center and solvent is not observed below 200 K because of "freezing in" of the protein conformation. Helical segments of the protein cannot move relative to one another, and rotational motions of the side chains are restricted. Absorption of visible light photons by the heme *a* and a_3 results in transient excited states. The absorbed energy is dissipated as heat. The low-spin cytochrome *a* heme iron is coordinated to two axial histidines, and its photoexcited heme is expected to rapidly relax to the ground state and result in a null vibrational difference spectrum under conditions of our measurements. It appears unlikely that any of the vibrational perturbations may be assigned to heme *a*, because relaxation of its photoexited heme is expected to be complete in the submicrosecond (or picosecond) time frame, long before the present observations were begun. Geminate recombination of the photolyzed iron-histidine bond was observed to occur in less than 20 ps in both cytochrome b_5 and cytochrome *c* by Jongeward et al. (1988). No groups in the protein other than heme A absorb visible light and thus would not be perturbed. The low temperature precludes motions of the protein, except as required for dissipation of the kinetic energy that results from absorption of a photon by the heme.

Correlations of infrared photoperturbation spectra of cytochrome *c* oxidase CO complex with resonance Raman spectra of oxidase derivatives and model compounds (Tables 1 and 2) suggest that FTIR absorbance difference spectroscopy can distinguish contributions from cytochrome a_3 heme without interference from cytochrome a, and in addition monitor the proximal histidine of cytochrome a_3 and histidines coordinated to Cu_B. The most clearly defined bands are due to the 8-formyl group at 1662 cm^{-1} and the 4-vinyl bending mode at 1082 cm^{-1}. The band near 1670–1674 cm^{-1} may be due to a small fraction of the sample that was not fully reduced by CO gas, but remained as a mixed valence (aFe(III)a_3Fe(II)CO..Cu_B). Photodissociation of CO may result in reverse electron transfer with formation of (aFe(II)a_3Fe(III)..Cu_BCO). The resonance

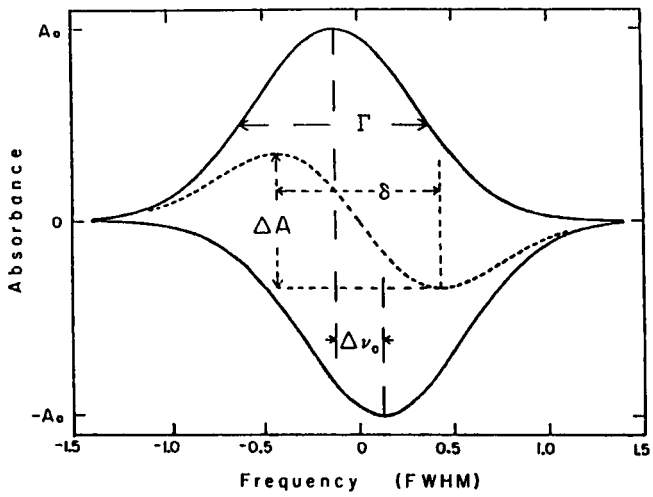

FIGURE 5 Absorbance difference spectrum (– – –) of two Gaussian bands (——) with identical half-widths, Γ (FWHH), normalized to the same peak intensity A_o, but separated in frequency by $\Delta\nu_o$. The peak-to-trough absorbance difference is ΔA, and the frequency difference is δ. The frequency scale is normalized to the half-width. From Alben and Fiamingo (1984).

Raman formyl transition of oxidized cytochrome *c* oxidase (Choi et al., 1983) was reported at 1676 cm^{-1}.

Perturbation of vibrational modes due to imidazole are expected from two sources: the proximal histidine coordinated to cytochrome a_3Fe, and histidines coordinated to Cu_B. Correlations in Tables 1 and 2 suggest that whereas most photoperturbed histidine vibrational modes contain overlapped contributions from a_3Fe and/or Cu_B complexes with porphyrin modes, band 24 at 1434 cm^{-1} may be a spectrally isolated mode due to the Cu_B-histidine complex, whereas band 44 at 1236 cm^{-1} is sensitive to axial ligation and is indicative of the His:a_3Fe:CO complex. Bands 36, 40, and 54 appear to contain contributions from both photoperturbed metal-histidine complexes. The correlations suggested in Tables 1 and 2 are not definitive, but should suggest spectral regions that require more rigorous testing of assignments.

The data reported here in sequential experiments on the identical sample of purified cytochrome *c* oxidase help to define the molecular changes that occur with photodissociation of the CO complex at 10–20 Kelvin. The purified oxidase appears to be identical in the CO stretching region to that previously reported for bovine heart mitochondrial preparations, and differs from the oxidase in rat myocyte or beef heart tissue preparations only in the ratio of beta to alpha forms (Fiamingo et al., 1982, 1986). The observations of midinfrared absorbance difference spectra, newly presented here, confirm that major perturbations occur at the cytochrome a_3-heme upon photodissociation, even at 10–20 Kelvin. Frequency-shifted bands have been assigned to porphyrin vibrational modes of heme a_3, to the 8-formyl and 4-vinyl substituent groups, to the proximal histidine coordinated to the a_3Fe, and to histidines coordinated to Cu_B. Additional frequency-shifted bands may be due to methyl and methylene substituents of the a_3-heme.

The present data provide new insight into the photodissociation process. Not only does the a_3Fe-coordinated CO receive enough kinetic energy to reach the adjacent Cu_B, but the a_3-heme is perturbed in a manner consistent with the expected change from a low-spin ($S = 0$) to a high-spin ($S = 2$) iron, and conversion of a tetragonal to a square-pyramidal heme complex. The observed increase in frequencies of the 8-formyl νC=O and 4-vinyl νC=C bands with photodissociation are consistent with decreased overlap of the pyrrole nitrogen p_π with iron d_{xz} and d_{yz} orbitals. This results in a decreased peripheral polarization of the heme and a decreased negative charge on the peripheral substituents, with the concomitant increase in C=O and C=C stretching frequencies. The foregoing changes in heme polarization with photodissociation of CO are analogous to effects on νCO of axially coordinated carbon monoxide that result from differences in polarization by porphyrin or axial ligand substituent groups transmitted through the iron in either the *cis* or *trans* directions (Alben and Caughey, 1968). They are also consistent with a high-spin iron in the photodissociated state observed by time-resolved magnetic circular dichroism of beef cytochrome *c* oxidase and by magnetic circular dichroism in cytochrome ba_3 from *Thermus thermophilus* (Goldbeck et al., 1992). These data are not consistent with the formation of a low-spin heme a_3 complex by a strong field ligand such as imidazole, but do not rule out a weak sigma-donor ligand such as water in the photodissociated state.

SUMMARY

Cytochrome *c* oxidase, purified from bovine heart, has been studied by infrared absorbance difference spectroscopy of the CO complex and its photodissociation product at 10–20 Kelvin. Photoperturbation is expected to change heme a_3 from a six-coordinated, low-spin iron complex to a five-coordinated, high-spin state, as CO is transferred from heme a_3 to Cu_B. Sixty-five absorbance difference bands have been associated with change in band frequency or absorptivity. These bands identify molecular changes due to the photodissociation process. Nearly all frequencies of the 19 resonance Raman active bands of cytochrome *c* oxidase CO complex (Argade et al., 1985) are closely duplicated by the infrared absorbance difference spectra. This is expected if and only if the molecular symmetry of heme a_3 is reduced to C_{2v} rather than D_{4h}, as has been commonly assumed. Formyl and vinyl substituents of heme a_3 show large absorbance difference spectra with photodissociation of CO. Quantitative analysis of the formyl group difference spectrum indicated a frequency shift of less than 2 cm^{-1} with photodissociation. Additional photoperturbed bands have been associated with heme a_3 axial histidine and with Cu_B histidine ligands, and with methyl and methylene porphyrin ring substituents of heme a_3. Additional uni-

dentified infrared perturbation bands may indicate perturbations of the heme pocket with low temperature photodissociation.

This work was supported in part by grant DMB-8904614 (to JOA) from the National Science Foundation and grant GM-22532 (to SIC) from the National Institutes of Health, U.S. Public Health Service.

REFERENCES

Alben, J. O. 1978. Infrared spectroscopy of porphyrins. *In* The Porphyrins. D. Dolphin, editor. Academic Press, New York. 323–345.

Alben, J. O. 1996. Fourier transform infrared spectroscopy of enzyme systems. *In* Infrared Spectroscopy of Biomolecules. H. H. Mantsch and D. Chapman, editors. Wiley-Liss, New York. 19–37.

Alben, J. O., R. A. Altschuld, F. G. Fiamingo, and P. P. Moh. 1982a. Structure of the cytochrome oxidase (a3) heme pocket. Low temperature FTIR spectroscopy of the photolyzed CO complex. *In* Interaction Between Iron Proteins in Oxygen and Electron Transport. C. Ho, editor. Elsevier-North Holland, Amsterdam. 205–208.

Alben, J. O. and G. H. Bare. 1978. Fourier transform infrared spectroscopic study of molecular interactions in hemoglobin. *Appl. Optics.* 17: 2985–2990.

Alben, J. O., D. Beece, S. F. Bowne, W. Doster, L. Eisenstein, H. Frauenfelder, D. Good, J. D. McDonald, M. C. Marden, P. P. Moh, L. Reinisch, A. H. Reynolds, E. Shyamsunder, and K. T. Yue. 1982b. Infrared spectroscopy of photodissociated carboxymyoglobin at low temperatures. *Proc. Natl. Acad. Sci. USA.* 79:3744–3748.

Alben, J. O., and W. S. Caughey. 1968. An infrared study of bound carbon monoxide in the human red blood cell, isolated hemoglobin, and heme carbonyls. *Biochemistry.* 7:175–183.

Alben, J. O., S. S. Choi, A. D. Adler, and W. S. Caughey. 1973. Infrared spectroscopy of porphyrins. *Ann. N.Y. Acad. Sci.* 206:278–395.

Alben, J. O., and F. G. Fiamingo. 1984. Fourier transform infrared spectroscopy. *In* Optical Techniques in Biological Research. D. L. Rousseau, editor. Academic Press, Orlando. 133–179.

Alben, J. O., W. H. Fuchsman, C. A. Beaudreau, and W. S. Caughey. 1968. Substituted deuteroporphyrins. III. Iron(II) derivatives. Reactions with oxygen and preparations from chloro- and methoxohemins. *Biochemistry.* 7:624–635.

Alben, J. O., P. P. Moh, F. G. Fiamingo, and R. A. Altschuld. 1981. Cytochrome oxidase (a3) heme and copper observed by low temperature Fourier transform infrared spectroscopy of the CO complex. *Proc. Natl. Acad. Sci. USA.* 78:234–237.

Argade, P. V., Y-C. Ching, and D. L. Rousseau. 1985. Resonance Raman spectral isolation of the a and a3 chromophore in cytochrome oxidase. *Biophys. J.* 50:613–620.

Babcock, G. T., and P. M. Callahan. 1983. Redox-linked hydrogen bond strength changes in cytochrome a: implications for a cytochrome oxidase proton pump. *Biochemistry.* 22:2314–2319.

Babcock, G. T., and M. Wikstrom. 1992. Oxygen activation and the conservation of energy in cell respiration. *Nature.* 356:301–309.

Callahan, P. M., and G. T. Babcock. 1983. Origin of the cytochrome a absorption red shift: a pH-dependent interaction between its heme a formyl and protein in cytochrome oxidase. *Biochemistry.* 22:452–461.

Chan, S. I., and P. M. Li. 1990. Cytochrome c oxidase: understanding nature's design of a proton pump. *Biochemistry.* 29:1–12.

Ching, Y.-C., P. V. Argade, and D. L. Rousseau. 1985. Resonance Raman spectra of CN-bound cytochrome oxidase: spectral isolation of cytochrome a^{2+}, a_3^{2+}, and a_3^{2+}CN. *Biochemistry.* 24:4938–4946.

Choi, S., J. J. Lee, Y. H. Wei, and T. G. Spiro. 1983. Resonance Raman and electronic spectra of heme a complexes and cytochrome oxidase. *J. Am. Chem. Soc.* 105:3692–3707.

Choi, S., T. G. Spiro, K. C. Langry, and K. M. Smith. 1982a. Vinyl influences on protoheme resonance Raman spectra: nickel(II) protoporphyrin IX with deuterated vinyl groups. *J. Am. Chem. Soc.* 104: 4337–4344.

Choi, S., T. G. Spiro, K. C. Langry, K. M. Smith, D. L. Budd, and G. N. La Mar. 1982b. Structural correlations and vinyl influences in resonance Raman spectra of protoheme complexes and proteins. *J. Am. Chem. Soc.* 104:4345–4351.

Cole, A. R. H. 1977. Tables of Wavenumbers for the Calibration of Infrared Spectrometers, Ed. 2. Pergamon Press, New York, for the International Union of Pure and Applied Chemistry, Commission on Molecular Structure and Spectroscopy.

Colombo, L., P. Bleckmann, B. Schrader, R. Schneider, and T. Plesser. 1974. Calculation of normal vibrations and intra- and intermolecular force constants in crystalline imidazole. *J. Chem. Phys.* 61:3270–3278.

de Paula, J. C., W. E. Peiffer, R. T. Ingle, J. A. Centeno, S. Ferguson-Miller, and G. T. Babcock. 1990. Hemes a and a3 environments of plant cytochrome c oxidase. *Biochemistry.* 29:8702–8706.

Dyer, R. B., O. Einarsdotter, P. M. Killough, J. J. Lopez-Garriga, and W. H. Woodruff. 1989. Transient binding of photodissociated CO to Cu_B^+ of eukaryotic cytochrome oxidase at ambient temperature. Direct evidence from time-resolved infrared spectroscopy. *J. Am. Chem. Soc.* 111: 7657–7659.

Fiamingo, F. G., R. A. Altschuld, and J. O. Alben. 1986. α and β forms of cytochrome c oxidase observed in rat heart myocytes by low temperature Fourier transform infrared spectroscopy. *J. Biol. Chem.* 261: 12976–12987.

Fiamingo, F. G., R. A. Altschuld, P. P. Moh, and J. O. Alben. 1982. Dynamic interactions of CO with a3Fe and CuB in cytochrome c oxidase in beef heart mitochondria studied by Fourier transform infrared spectroscopy at low temperatures. *J. Biol. Chem.* 257:1639–1650.

Garcia-Horsman, J. A., B. Barquera, J. Rumbley, J. Ma, and R. B. Gennis. 1994. The superfamily of heme-copper respiratory oxidases. *J. Bacteriol.* 176:5587–5600.

Goldbeck, R. A., O. Einarsdottir, T. D. Dawes, D. B. O'Conner, K. K. Surerus, J. A. Fee, and D. S. Kliger. 1992. Magnetic circular dichroism study of cytochrome ba3 from *Thermus thermophilus*: spectral contributions from cytochromes b and a3 and nanosecond spectroscopy of CO photodissociation. *Biochemistry.* 31:9376–9387.

Han, S., Y-C. Ching, S. L. Hammes, and D. L. Rousseau. 1991. Vibrational structure of the formyl group on heme a. Implications on the properties of cytochrome c oxidase. *Biophys. J.* 60:45–52.

Hartzell, C. R., and H. Beinert. 1974. Components of cytochrome c oxidase detectable by EPR spectroscopy. *Biochim. Biophys. Acta.* 368:318–338.

Iwata, S., C. Ostermeier, B. Ludwig, and H. Michel. 1995. Structure at 2.8 Å resolution of cytochrome c oxidase from *Paracoccus denitrificans*. *Nature.* 376:660–669.

Jongeward, K. A., D. Magde, D. J. Taube, and T. G. Traylor. 1988. Picosecond kinetics of cytochrome b5 and c. *J. Biol. Chem.* 263: 6027–6030.

Kitagawa, T., and Y. Ozaki. 1987. Infrared and Raman spectra of metalloporphyrins. *Struct. Bonding.* 64:71–114.

Laane, J. 1981. Determination of bandwidth and frequency changes by Raman difference spectroscopy. *J. Chem. Phys.* 75:2539–2545.

Laane, J., and W. Kiefer. 1980. Determination of frequency shifts by Raman difference spectroscopy. *J. Chem. Phys.* 72:5305–5311.

Ogura, T., S. Takahashi, K. Shinzawa-Itoh, S. Yoshikawa, and T. Kitagawa. 1990. Observation of the Fe^{4+}=O stretching Raman band for cytochrome oxidase compound B at ambient temperature. *J. Biol. Chem.* 265:14721–14723.

Pan, L.P., Z. Li, R. Larsen, and S. I. Chan. 1991. The nature of Cux in cytochrome c oxidase. *J. Biol. Chem.* 266:1367–1370.

Park, S., L-P. Pan, S. I. Chan, and J. O. Alben. 1992. The heme a3 8-formyl group observed by photoperturbation of cytochrome c oxidase CO complex at 10 Kelvin with Fourier transform infrared spectroscopy. *Biophys. J.* 61:A203. (Abstr.)

Rousseau, D. L. 1981. Raman difference spectroscopy as a probe of biological molecules. *J. Raman Spectrosc.* 10:94–99.

Salmeen, I., L. Rimai, D. Gill, T. Yamamoto, G. Palmer, C. R. Hartzell, and H. Beinert. 1973. Resonance Raman spectroscopy of cytochrome c oxidase and electron transport particles with excitation near the soret band. *Biochem. Biophys. Res. Commun.* 52:1100–1107.

Sassaroli, M., Y-C. Ching, P. V. Argade, and D. L. Rousseau. 1988. Photodissociated cytochrome c oxidase: cryotrapped metastable intermediates. *Biochemistry.* 27:2496–2502.

Tsukihara, T., H. Aoyama, E. Yamashita, T. Tomizaki, H. Yamaguchi, K. Shinzawa-Itoh, R. Nakashima, R. Yaono, and S. Yoshikawa. 1995. Structures of metal sites of oxidized bovine heart cytochrome c oxidase at 2.8 Å. *Science.* 269:1069–1074.

Walters, M. A., and T. G. Spiro. 1983. Resonance Raman enhancement of imidazole vibrations via charge-transfer transitions of pentacyanoiron(II) imidazole and imidazolate complexes. *Inorg. Chem.* 22: 4014–4017.

Wikstrom, M., K. Krab, and M. Saraste. 1981. Cytochrome Oxidase: A Synthesis. Academic Press, New York.

Wilson, M. T., T. Alleyne, M. Clague, K. Conroy, and B. El-Agez. 1988. Electron transfer and conformation states in bovine cytochrome c oxidase. *Ann. N.Y. Acad. Sci.* 550:167–176.

Woodruff, W. H., O. Einarsdottir, R. B. Dyer, K. A. Bagley, G. Palmer, S. J. Atherton, R. A. Goldbeck, T. D. Dawes, and D. S. Kliger. 1991. Nature and functional implications of the cytochrome a3 transients after photodissociation of CO-cytochrome oxidase. *Proc. Natl. Acad. Sci. USA.* 88:2588–2592.

Yoshikawa, S., M. G. Choc, M. C. O'Toole, and W. S. Caughey. 1977. An infrared study of CO binding to heart cytochrome c oxidase and hemoglobin A. *J. Biol. Chem.* 252:5498–5508.